

# External-cavity difference-frequency source near $3.2 \mu\text{m}$ , based on combining a tunable diode laser with a diode-pumped Nd:YAG laser in AgGaS<sub>2</sub>

U. Simon

*Department of Electrical and Computer Engineering, Rice University, Houston, Texas 77251-1892*

S. Waltman

*Time and Frequency Division, National Institute of Standards and Technology, 235 Broadway, Boulder, Colorado 80303*

I. Loa and F. K. Tittel

*Department of Electrical and Computer Engineering, Rice University, Houston, Texas 77251-1892*

L. Hollberg

*Time and Frequency Division, National Institute of Standards and Technology, 325 Broadway, Boulder, Colorado 80303*

Received April 29, 1994; revised manuscript received August 26, 1994

AgGaS<sub>2</sub> has been used to generate more than  $2 \mu\text{W}$  of cw mid-infrared radiation near  $3.2 \mu\text{m}$  by difference-frequency mixing of the outputs of an extended-cavity diode laser near  $795 \text{ nm}$  (pump wave) and a compact diode-pumped Nd:YAG laser at  $1064 \text{ nm}$  (signal wave). An external ring enhancement cavity was used to build up the signal power inside the nonlinear crystal by as much as 14.5 times. The novel mid-infrared source incorporating a single diode laser could be angle-tuned from  $3.155$  to  $3.423 \mu\text{m}$  (from  $3170$  to  $2921 \text{ cm}^{-1}$ ). This system was used to detect the Doppler-broadened fundamental  $\nu_3$ -asymmetric stretch vibration of methane (CH<sub>4</sub>) by both direct and wavelength-modulation absorption spectroscopy.

## 1. INTRODUCTION

Difference-frequency generation (DFG) of continuous-wave (cw) tunable infrared single-frequency radiation has proved to be a useful technique for high-resolution infrared spectroscopy but was limited until recently to wavelengths shorter than  $5 \mu\text{m}$  by the infrared transmission characteristics of the available nonlinear optical materials (LiNbO<sub>3</sub> and LiIO<sub>3</sub>).<sup>1</sup> Recent advances in the growth and the fabrication of nonlinear optical materials, such as AgGaS<sub>2</sub> and AgGaSe<sub>2</sub>, now offer a convenient means for extending the wavelength coverage of DFG sources to a wider wavelength range ( $3$ – $18 \mu\text{m}$ ).<sup>2,3</sup>

Semiconductor diode lasers are particularly attractive as pump sources in the nonlinear DFG process, as their compact size and ease of operation will permit the construction of portable and robust mid-infrared laser sources that are especially suitable for environmental remote sensing, pollution monitoring, chemical analysis, and medical research. Until now the nonlinear frequency conversion efficiency of all-diode-laser DFG sources has been limited by the relatively low output power of commercially available single-mode III–V diode lasers. We reported several nanowatts of cw mid-infrared radiation<sup>4</sup> near  $5 \mu\text{m}$ , obtained by difference-frequency mixing of two visible–near-infrared diode lasers ( $2$  and  $10 \text{ mW}$ ) in AgGaS<sub>2</sub>. Using KTP as the nonlinear optical material, Wang and Ohtsu<sup>5</sup> generated

as much as  $300 \text{ nW}$  of near-infrared radiation ( $\sim 1.6 \mu\text{m}$ ) from two diode lasers ( $50 \text{ mW}$  each). One way to increase the infrared DFG output power is to use optical semiconductor amplifiers to boost the power of the single-mode diode lasers to the watt level. Recently we demonstrated difference-frequency mixing of a high-power, GaAlAs, tapered, traveling-wave, semiconductor amplifier<sup>6</sup> with a cw Ti:Al<sub>2</sub>O<sub>3</sub> laser in a  $45\text{-mm}$ -long AgGaS<sub>2</sub> crystal cut for type-I noncritical phase matching at room temperature. The diode amplifier was injection seeded by a low-power, single-mode, index-guided diode laser and provided  $1.5 \text{ W}$  of  $860\text{-nm}$  radiation for the DFG mixing experiment. As much as  $47 \mu\text{W}$  of cw infrared radiation and  $89 \mu\text{W}$  of pulsed infrared radiation, tunable near  $4.3 \mu\text{m}$ , was generated. Alternatively, the infrared DFG output power can be increased by use of the high circulating fields inside optical resonators with the nonlinear crystal placed either in an external (passive) enhancement cavity or in one of the pump-laser cavities. The latter approach was investigated by Dixon and co-workers<sup>7</sup> with a nonlinear KTP or AgGaS<sub>2</sub> crystal introduced into a Nd:YAG laser cavity.

In this paper we describe a DFG source that uses a tunable extended-cavity diode laser (ECDL) near  $795 \text{ nm}$  ( $500\text{-kHz}$  linewidth), a diode-pumped monolithic Nd:YAG laser at  $1064 \text{ nm}$  ( $5\text{-kHz}$  linewidth), and an external ring enhancement cavity around a AgGaS<sub>2</sub> crystal. The enhancement cavity resonates the signal wavelength

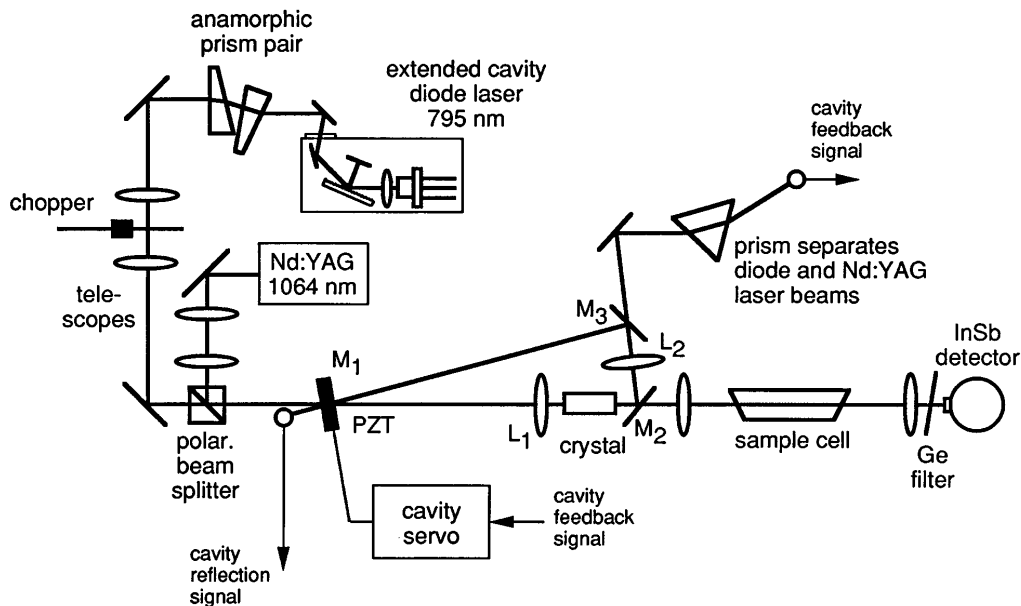


Fig. 1. Experimental setup used to mix the outputs of an ECDL near 795 nm and a diode-laser-pumped Nd:YAG laser at 1064 nm in AgGaS<sub>2</sub> cut for 90° type-I phase matching. The Nd:YAG laser radiation inside the mixing crystal is resonantly enhanced by a three-mirror ring buildup cavity.

(Nd:YAG laser), thereby increasing the signal power present inside the mixing crystal. The infrared power scales as the product of the signal and the pump powers, and hence its enhancement depends linearly on the buildup factor.

## 2. EXPERIMENTAL SETUP

The experimental diagram in Fig. 1 shows the ring buildup cavity, the ECDL, and the diode-pumped Nd:YAG laser. The ECDL<sup>8</sup> uses an index-guided, quantum-well laser,<sup>9</sup> a 0.60 N.A. collimating objective, and a reflection grating (2400 lines/mm) used in the Littman configuration. To improve the tuning characteristics of the ECDL, the output facet of the laser chip was antireflection (AR) coated with Al<sub>2</sub>O<sub>3</sub> and HfO<sub>2</sub>. Most high-power diode lasers are supplied from the manufacturer with reduced-reflectance coatings on the front facet and high-reflectance coatings on the back facet. These standard high-power lasers will work well in an ECDL configuration, but further reduction of the front facet reflectance permits a broader tuning range. An anamorphic prism pair (6×) and a telescope were used to match the spatial mode of the ECDL approximately to the Nd:YAG laser mode in the ring buildup resonator.

The signal wave was provided by a cw diode-pumped monolithic Nd:YAG ring laser<sup>10</sup> at 1064 nm. Pump- and signal-wave polarizations were perpendicular for type-I phase matching in AgGaS<sub>2</sub>. Both beams were spatially overlapped with a polarizing beam splitter. Telescopes were used in both beam paths to match the beam waists at the center of the crystal. The beam waists (half-width at 1/e<sup>2</sup> of maximum) were set to ~20 μm in both vertical and horizontal planes, which is close to optimum focusing.<sup>2</sup>

To minimize thermal effects on the nonlinear conversion efficiency, the signal wave at 1064 nm rather than the pump wave at 795 nm was resonated in the

buildup cavity. Owing to poor thermal conductivity (~0.115 W cm<sup>-1</sup> K<sup>-1</sup>), AgGaS<sub>2</sub> suffers from thermal lensing problems, especially if high-power pump sources at wavelengths close to the absorption-band edge of the material (~500 nm) are used.<sup>11</sup> Both to avoid degradation of the wave fronts by thermal lensing effects and to have a broad angle tuning range, we chose a short AgGaS<sub>2</sub> mixing crystal (5 mm long) in this experiment. After AR coatings were applied to the crystal facets, the total linear absorption loss of the AgGaS<sub>2</sub> crystal at 1064 nm was measured to be ~1.5%.

The ring buildup cavity consisted of three flat mirrors (M<sub>1</sub>–M<sub>3</sub>) and two intracavity lenses (L<sub>1</sub>,  $f_{L_1} = 50$  mm; L<sub>2</sub>,  $f_{L_2} = 25$  mm) together with a 5-mm-long AgGaS<sub>2</sub> crystal cut for type-I 90° phase matching. With a crystal aperture of 5 mm this configuration gave us access to phase-matching angles between 90° and 67°. The total length of the ring cavity was ~28 cm, and the full angle  $\Theta$  on mirror M<sub>1</sub> was ~3°. The facets of the nonlinear mixing crystal were coated with a single-layer Al<sub>2</sub>O<sub>3</sub> AR coating for low loss at 1064 nm ( $R \approx 4 \times 10^{-5}$ ). In spite of the quality of the coatings, passive losses from the lenses ( $R < 0.25\%$  per surface, nominally) reduced the cavity buildup. However, the cavity setup shown in Fig. 1 could be realized almost exclusively with standard Nd:YAG laser optics. Mirrors M<sub>2</sub> and M<sub>3</sub> were high-reflectance coated (nominally  $R \sim 98.5\%$  and  $R \sim 99.7\%$ , respectively) for *s*-polarized light at 1064 nm. The infrared radiation generated inside the crystal was coupled out through mirror M<sub>2</sub>, which was an Al<sub>2</sub>O<sub>3</sub> substrate high-reflectance coated for 1064 nm with transmission  $T \approx 78\%$  for the generated difference-frequency radiation near 3 μm. Mirror M<sub>1</sub> was used as the input coupler, with  $T \approx 4\%$  (nominally) at 1064 nm chosen to impedance match<sup>12</sup> the buildup cavity to the signal-wave losses. Approximately 85% of the diode laser power at 795 nm incident upon the cavity could be coupled through M<sub>1</sub>.

### 3. RESULTS AND DISCUSSION

With no mixing crystal inside the buildup cavity, approximately 75% of the incident Nd:YAG laser power was coupled into the cavity and enhanced by a factor of  $\sim 24.5$ , corresponding to a total cavity round-trip loss of  $\sim 4.1\%$ . After the crystal was introduced into the cavity, the coupling increased to  $\sim 83\%$ , indicating a better match of the input coupler transmission to the total cavity round-trip loss. However, owing to the additional absorption of the mixing crystal, the buildup factor decreased to  $\sim 14.5$ , corresponding to a total cavity round-trip loss of  $\sim 6.9\%$ .

The coupling efficiency of the Nd:YAG laser power into the buildup cavity was determined from the power reflected off the input coupler  $M_1$  while the buildup cavity was tuned over the resonance with the piezoelectric-transducer- (PZT-) driven mirror  $M_1$ . The circulating power inside the cavity could be inferred from the Nd:YAG laser power that leaked through mirror  $M_3$ . After traversing a  $60^\circ$  prism that separated the Nd:YAG laser beam from the diode laser beam, the transmitted signal was also used to lock the cavity resonance to the Nd:YAG laser frequency with a standard modulation-control scheme.

The difference-frequency radiation generated in the AgGaS<sub>2</sub> crystal was collimated outside the buildup cavity with a CaF<sub>2</sub> lens (5-cm focal length) and then detected by a liquid-N<sub>2</sub>-cooled photovoltaic detector (InSb with a 1-mm-diameter area and a factory calibrated responsivity of  $\sim 1.248$  A/W at  $3\ \mu\text{m}$ ). A broadband AR-coated germanium filter blocked pump and signal waves while transmitting the  $3\text{-}\mu\text{m}$  difference-frequency radiation.

Using 1064.504 nm as the signal wave, we found type-I  $90^\circ$  phase matching at a diode laser wavelength of 795.5 nm, corresponding to a difference-frequency wavelength of  $\sim 3.148\ \mu\text{m}$  ( $3176.7\ \text{cm}^{-1}$ ). The laser wavelengths were determined with a spectral resolution of  $\sim 30$  MHz and an absolute accuracy of  $\sim 500$  MHz with the radiation coupled via a single-mode probe fiber into a lambdameter.<sup>13</sup> The DFG phase-matching bandwidth at a phase-matching angle of  $90^\circ$  is shown in Fig. 2. This was recorded by tuning the wavelength of the ECDL. The large phase-matching bandwidth of  $\sim 8.8\ \text{cm}^{-1}$  (FWHM) is in good agreement with the theoretically calculated value of  $8.1\ \text{cm}^{-1}$ , which results mainly from the short length (5 mm) of the nonlinear optical mixing crystal.

Figure 3 depicts the mid-infrared DFG power at  $90^\circ$  phase matching for a fixed diode-laser power of 12.1 mW (measured after the input coupler of the buildup cavity) as a function of the Nd:YAG laser power incident upon the enhancement cavity. The Nd:YAG laser power was varied by the relative angle between a polarization rotator and an analyzer. Values shown are corrected for the  $3\text{-}\mu\text{m}$  transmission loss of the optical components external to the cavity ( $T \approx 89\%$ ), but not for the transmission loss of the infrared light in the output coupler of the buildup cavity ( $T \approx 78\%$ ). The plot shows the expected linear dependence of the generated infrared power on the signal power. However, the experimentally determined slope efficiency of  $\sim 4.1\ \text{nW/mW}$  at 12.1 mW of diode laser power is approximately four times less than the value

that was predicted based on the theoretical model (given in Refs. 2 and 3) assuming ideal Gaussian beams and an effective nonlinear coefficient of  $12 \times 10^{-12}$  m/V for type-I  $90^\circ$  phase matching in AgGaS<sub>2</sub>. This deviation between experiment and theory was also found in previous AgGaS<sub>2</sub> DFG experiments.<sup>6</sup> A maximum cw DFG power of  $\sim 1.7\ \mu\text{W}$  was obtained after the external cavity with  $\sim 13.6$  mW of diode laser power and 360 mW of Nd:YAG laser power. Taking into account the buildup cavity output coupler transmission at  $3\ \mu\text{m}$ , this corresponds to  $\sim 2.1\ \mu\text{W}$  of DFG power after the mixing crystal. Even at the high-signal-power levels circulating inside the buildup cavity, the infrared DFG power was the same for both cw and pulsed modes of operation. For cw operation the buildup cavity resonance was locked to

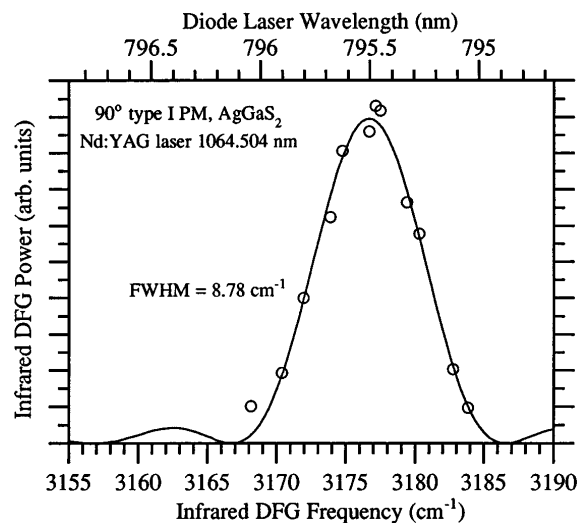


Fig. 2. Phase-matching bandwidth of the DFG mixing process at a phase-matching angle of  $90^\circ$ , recorded with the diode laser wavelength tuned. The large bandwidth of  $>8\ \text{cm}^{-1}$  (FWHM) is due to the 5-mm length of the crystal used in the nonlinear optical mixing.

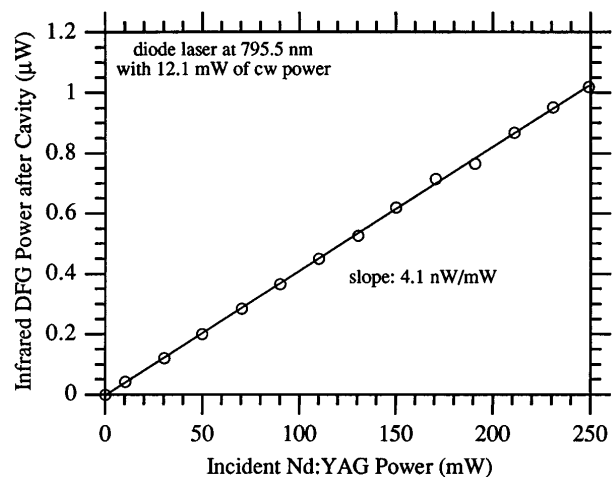


Fig. 3. Generated infrared DFG power as a function of the Nd:YAG laser power incident upon the enhancement cavity. For this measurement the diode laser power was fixed at 12.1 mW (measured after the input coupler of the buildup cavity). Values shown are corrected for transmission losses of the optical components external to the buildup cavity at a wavelength of  $3\ \mu\text{m}$ .

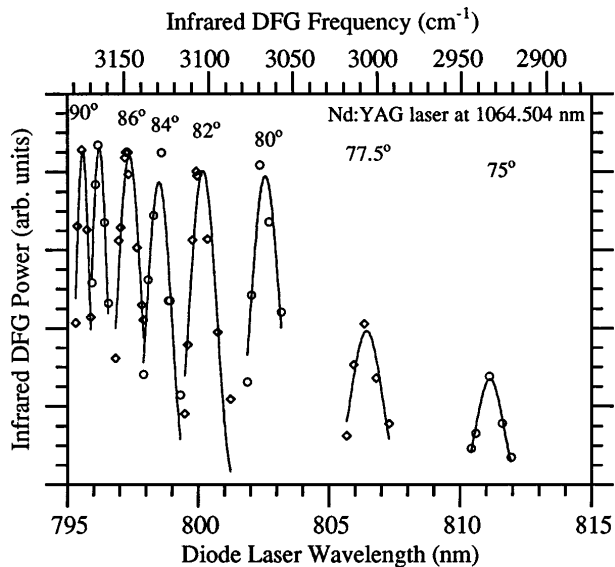


Fig. 4. Tuning range and power output of the infrared DFG radiation. Infrared tuning was accomplished by variation of the wavelength of the diode laser for a given orientation of the mixing crystal.

the Nd:YAG laser while pulsed operation was obtained by sweeping the cavity over its resonance in  $\sim 0.4$  ms and detecting the transmitted infrared signal. This indicates that, even at circulating power levels of  $>3.5$  W inside the cavity, no degradation of the nonlinear conversion efficiency by thermal lensing effects was observed.

With the wavelength of the ECDL tuned from 795 to 812 nm (over  $\sim 17$  nm) and the phase-matching angle of the mixing crystal adjusted (over  $\sim 15^\circ$ ), the infrared wavelength could be tuned from 3.155 to 3.423  $\mu\text{m}$  ( $3170\text{--}2921\text{ cm}^{-1}$ ). Figure 4 shows the relative infrared DFG power as a function of the diode laser and infrared wavelengths over the entire tuning range of the diode laser. We recorded the tuning curve by setting the phase-matching angle to a given value and tuning the diode laser over the DFG phase-matching bandwidth. The DFG power levels shown here are normalized to the incident diode-laser power, which varied from 10 to 15 mW over this tuning range. We achieved continuous infrared tuning ranges of  $>40$  GHz without mode hopping by scanning the piezoelectric transducer on the ECDL. Figure 4 indicates that for phase-matching angles above  $80^\circ$  the effective phase-matching length<sup>14</sup> is actually larger than the physical length of the mixing crystal, which results in a nearly constant infrared DFG power between  $90^\circ$  and  $80^\circ$ . For phase-matching angles smaller than  $80^\circ$  the effective phase-matching length drops below the physical length of the crystal because of walk-off effects, resulting in an equivalent drop of the generated infrared power. Figure 5 shows the experimentally measured phase-matching points compared with the values theoretically calculated from the Sellmeier coefficients given in Ref. 15. Rotating the nonlinear crystal in the buildup cavity introduced a shift of the laser beams. Therefore at each crystal angle a realignment of the cavity was required. This can be avoided, however, by use of two crystals in a walk-off compensated cavity configuration as demonstrated by Bosenberg *et al.*<sup>16</sup>

To demonstrate the applicability of this compact all-solid-state DFG source, we recorded a portion of the absorption spectrum of the fundamental  $\nu_3$ -asymmetric stretch vibration of methane ( $\text{CH}_4$ ) around 3.2  $\mu\text{m}$  (see Fig. 6). The phase-matching angle was set to  $90^\circ$  and the ECDL wavelength was tuned over an  $\sim 30$ -GHz portion of the DFG phase-matching bandwidth. Only 100 mW of incident Nd:YAG laser power was used to record this spectrum, which corresponds to an infrared power level of  $\sim 0.45\text{ }\mu\text{W}$ . The methane pressure in the 50-cm-long absorption cell was set to the vapor pressure of methane at 77 K (1333 Pa, 10 Torr) with a liquid- $\text{N}_2$ -cooled reservoir. Figure 6 depicts a portion of the recorded methane absorption spectrum and demonstrates the high signal-to-noise ratios that could readily be obtained. Trace 1 of Fig. 6 shows a (single-sweep) background-free absorption spectrum recorded by wavelength modulation of the diode laser (cavity length), with the  $2f$ -absorption signal detected by lock-in techniques. Trace 2 of Fig. 6 shows

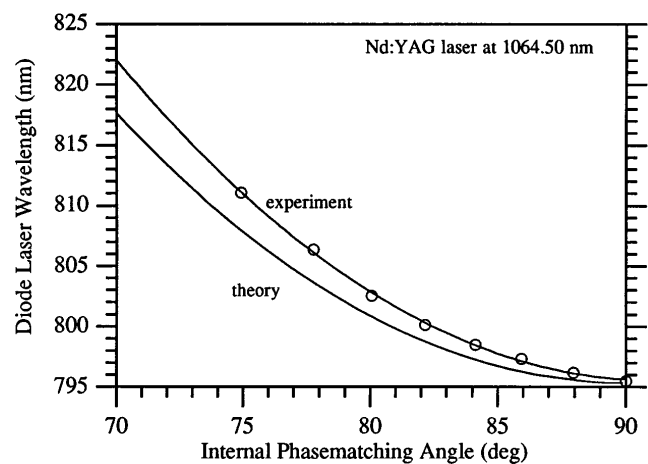


Fig. 5. Comparison of the experimentally determined (data points, circles; fit, top solid curve) and theoretically calculated (bottom curve) phase-matching angles. The calculated values are based on the Sellmeier equations given in Ref. 15.

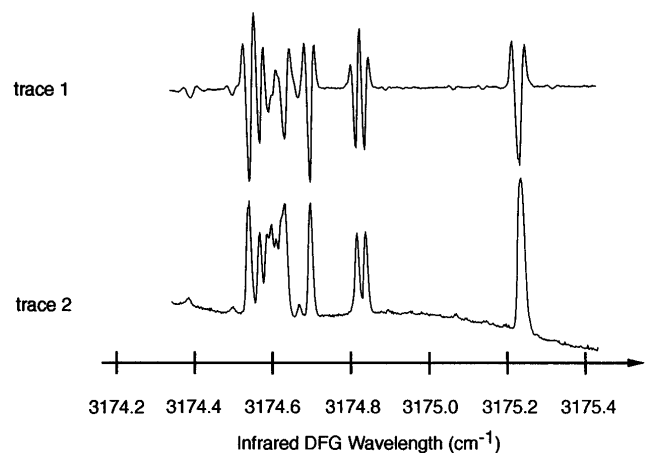


Fig. 6. Methane absorption spectrum near 3.2  $\mu\text{m}$  (fundamental  $\nu_3$ -asymmetric stretching motion), obtained with a 50-cm-long absorption cell and a methane pressure of  $\sim 10$  Torr. Trace 1,  $2f$ -absorption signal (single sweep) recorded with a lock-in amplifier. The spectrum was recorded at a phase-matching angle of  $90^\circ$  with the diode laser wavelength tuned over a 30-GHz portion of the phase-matching bandwidth; trace 2, a direct absorption signal obtained by the averaging of 10 sweeps.

the direct absorption spectrum of the same lines recorded with a digital oscilloscope averaging 10 sweeps. The buildup cavity was resonant only at 1064 nm, with no measurable buildup at the diode laser wavelength. Thus no channeling on the baseline of the methane spectrum was observed when the diode laser wavelength was tuned.

#### 4. CONCLUSION

In conclusion, more than 2  $\mu\text{W}$  of cw tunable infrared radiation near 3.2  $\mu\text{m}$  have been generated by difference-frequency mixing an ECDL (pump source) near 795 nm and a diode-pumped Nd:YAG laser (signal source) in AgGaS<sub>2</sub>. The signal source was resonated in a ring enhancement cavity, resulting in buildup factors for the signal power of as much as 14.5. The compact infrared DFG source (footprint of 0.5 m<sup>2</sup>) could be tuned from 3.155 to 3.423  $\mu\text{m}$  (3170 to 2921 cm<sup>-1</sup>), which coincides with the fundamental CH stretch vibrations of the vast majority of molecular organic compounds. The DFG source was used to detect the fundamental  $\nu_3$ -asymmetric stretching motion of methane by direct and modulation spectroscopy. Methane was chosen in this feasibility study because of its convenience and its environmental significance (it is an important greenhouse gas that supports ozone formation in polluted air). With the Nd:YAG laser line at 1.32  $\mu\text{m}$  as the signal wave and a tunable high-power ECDL near 855 nm as the pump wave, angle-tunable mid-infrared radiation from 2.42 to 2.57  $\mu\text{m}$  (phase-matching angles 90–75°) could be generated. The cavity-enhanced DFG source demonstrated here is a useful system whenever low power consumption, relatively low cost, and no-water cooling are important and for wavelength regions in which high-power semiconductor GaAlAs optical amplifiers<sup>6</sup> are not available. This makes it an attractive tool for wide range of applications in the mid-infrared wavelength range.

#### ACKNOWLEDGMENTS

This work has been supported in part by the Robert A. Welch Foundation, the National Science Foundation, the U.S. Air Force Office of Scientific Research, and NASA. The authors thank J. L. Hall for significant contributions and Lightwave Electronics, Inc., for providing the diode-pumped Nd:YAG laser<sup>10</sup> used in this work. U. Simon gratefully acknowledges the support of the A. v. Humboldt-Foundation by a F. Lynen Fellowship.

#### REFERENCES AND NOTES

1. A. S. Pine, "Doppler-limited molecular spectroscopy by difference-frequency mixing," *J. Opt. Soc. Am.* **64**, 1683

- (1974); M. G. Bawendi, B. D. Rehfuss, and T. Oka, "Laboratory observation of hot bands of H<sub>3</sub><sup>+</sup>," *J. Chem. Phys.* **93**, 6200 (1990).
2. P. Canarelli, Z. Benko, R. F. Curl, and F. K. Tittel, "A continuous-wave infrared laser spectrometer based on difference-frequency generation in AgGaS<sub>2</sub> for high-resolution spectroscopy," *J. Opt. Soc. Am. B* **9**, 197 (1992).
3. A. H. Hielscher, C. E. Miller, D. C. Bayard, U. Simon, K. P. Smolka, R. F. Curl, and F. K. Tittel, "Optimization of a midinfrared high-resolution difference-frequency laser spectrometer," *J. Opt. Soc. Am. B* **9**, 1962 (1992).
4. U. Simon, C. E. Miller, C. C. Bradley, R. G. Hulet, R. F. Curl, and F. K. Tittel, "Difference-frequency generation in AgGaS<sub>2</sub> by use of single-mode diode-laser pump sources," *Opt. Lett.* **18**, 1062 (1993).
5. W. Wang and M. Ohtsu, "Frequency-tunable sum- and difference-frequency generation by using two diode lasers in a KTP crystal," *Opt. Commun.* **102**, 304 (1993).
6. U. Simon, F. K. Tittel, and L. Goldberg, "Difference-frequency mixing in AgGaS<sub>2</sub> by use of a high-power GaAlAs tapered semiconductor amplifier at 860 nm," *Opt. Lett.* **18**, (1993).
7. F. J. Effenberger and G. J. Dixon, "2.95  $\mu\text{m}$  intracavity difference-frequency laser," in *Digest of Topical Meeting on Advanced Solid State Lasers* (Optical Society of America, Washington, D.C., 1992), p. 59; "Intracavity difference frequency generation," in *Lasers and Electro-Optics*, Vol. 8 of 1994 OSA Technical Digest Series (Optical Society of America, Washington, D.C., 1994), p. 380.
8. C. E. Wieman and L. Hollberg, "Using diode lasers in atomic physics," *Rev. Sci. Instrum.* **62**, 1 (1991).
9. SDL, Inc., Model SDL5410C (mentioned to help to specify experimental parameters; other sources may be suitable).
10. Lightwave Electronics, Inc., Model 122-1064-500-F, 500 mW (mentioned to help to specify experimental parameters; other sources may be suitable).
11. C. E. Miller, W. C. Eckhoff, U. Simon, F. K. Tittel, and R. F. Curl, "Difference-frequency laser spectrometer using AgGaS<sub>2</sub>: problems encountered in power scaling," in *Nonlinear Optics for High-Speed Electronics and Optical Frequency Conversion*, N. Peyghambarian, H. Everitt, and R. C. Eckardt, eds., *Proc. Soc. Photo-Opt. Instrum. Eng.* **2145**, 282 (1994).
12. W. J. Kozlovsky, C. D. Nabors, and R. L. Byer, "Efficient second harmonic generation of a diode-pumped cw Nd:YAG laser using monolithic MgO:LiNbO<sub>3</sub> external resonant cavities," *J. Quantum Electron.* **24**, 913 (1988).
13. J. L. Hall and S. A. Lee, "Interferometric real-time display of cw dye laser wavelength with sub-Doppler accuracy," *Appl. Phys. Lett.* **29**, 367 (1976).
14. R. L. Byer and R. L. Herbst, "Parametric oscillation and mixing," in *Nonlinear Infrared Generation*, V. R. Shen, ed. (Springer-Verlag, New York, 1977), pp. 81–137.
15. Y. X. Fan, R. C. Eckardt, R. L. Byer, R. K. Route, and R. S. Feigelson, "AgGaS<sub>2</sub> infrared parametric oscillator," *Appl. Phys. Lett.* **45**, 313 (1984).
16. W. R. Bosenberg, W. S. Pelouch, and C. L. Tang, "High-efficiency and narrow-linewidth operation of a two-crystal  $\beta$ -BaB<sub>2</sub>O<sub>4</sub> optical parametric oscillator," *Appl. Phys. Lett.* **55**, 1952 (1989).